CHEMISTRY
A EUROPEAN JOURNAL

DOI: 10.1002/chem.200601087

Arene Complexes of β-Diketiminato Supported Organoscandium Cations: Mechanism of Arene Exchange and Alkyne Insertion in Solvent Separated Ion Pairs

Paul G. Hayes,[a, b] Warren E. Piers,*[a] and Masood Parvez[a]

Abstract: A family of isolable solvent separated organoscandium methyl cations stabilized by β-diketiminato ligands (Ar)NC(CH_3)CHC(CH_3)N(Ar) (Ar = 2,6-*i*Pr-C_6H_3, L^{Me}) has been prepared by reaction of $L^{Me}ScR_2$ with $[CPh_3][B(C_6F_5)_4]$ in the presence of an arene solvent. Arenes such as bromobenzene, benzene, toluene, *para*-xylene and mesitylene bind the scandium center in an η^6-bonding mode, yielding cations **1a–e**. Their solution and solid-state structures have been explored using multinuclear NMR spectroscopy and X-ray crystallography. Mechanistic studies on arene exchange reactions and the insertion of diphenylacetylene indicate that these processes occur via arene intermediates of lower hapticity, followed by binding of the incoming reagent. Which of the two steps is rate limiting depends on the arene being displaced and/or the nature of the incoming substrate. The experiments present a unified view of these mechanisms, which have relevance to propagation processes in olefin polymerizations mediated by such cations.

Keywords: arenes · ion pairs · polymerization · scandium

Introduction

The role of highly electrophilic, early transition-metal organocations in olefin polymerization is well established.[1] Access to these reactive species usually involves the activation of a neutral dialkyl catalyst precursor via an alkide abstraction process,[2] and catalyst efficiency is, generally speaking, dictated by the inherent activity of the catalyst, its thermal stability towards deactivation processes and the proportion of catalyst which is active at any given time. These phenomena often interfere with each other; for example, sterically more open catalysts that are more active, are often more prone to deactivation, particularly at low monomer concentrations, or solvent coordination to produce dormant catalyst states.[1]

[a] Prof. P. G. Hayes, Prof. W. E. Piers, Dr. M. Parvez
Department of Chemistry, University of Calgary
2500 University Dr. NW, Calgary, Alberta T2N 1N4 (Canada)
Fax: (+1) 403-289-9488
E-mail: wpiers@ucalgary.ca

[b] Prof. P. G. Hayes
Present Address:
Department of Chemistry and Biochemistry
University of Lethbridge, E866, University Hall
Lethbridge, Alberta, T1K 3M4 (Canada)

Supporting information for this article is available on the WWW under http://www.chemeurj.org/ or from the author.

These issues have come to light more prominently in the development of so-called "post-metallocene" catalysts.[3] Among the first examples of such catalysts were McConville's bisamido titanium compounds that, although able to polymerize ethylene in a living fashion,[4] were prone to deactivation processes brought on by C–H activation[5] and severe decrease in activity in the presence of weak donors, even toluene.[4] Thus, the progression to more open-ligand environments, aimed at increasing activity, restricts the conditions under which the active catalyst may be generated and problems with several common activators begin to surface at this developmental front. For example, the strong Lewis acid $B(C_6F_5)_3$[6] produces highly active contact ion pairs (CIPs) prone to back transfer of -C_6F_5,[2] frequently yielding inactive M-C_6F_5 species.[7] Use of common protic activators such as $[HNMe_2Ph][B(C_6F_5)_4]$[8] or $[H(OEt_2)_2][B(C_6F_5)_4]$[9] gives cations that detrimentally coordinate the NMe_2Ph and OEt_2 conjugate bases.[10,11] The trityl borate activator $[Ph_3C][B(C_6F_5)_4]$[12] does not have either of these problems,[13] but if the cations produced are sufficiently sterically open, the coordination of solvent molecules to give solvent separated ion pairs (SSIPs) can weaken the ability of the catalyst to take up monomer.

It is clear that the nature of the ion pair (CIP vs SSIP) and the cation's interactions with its environment are defining factors in the catalyst behavior.[14] While CIPs have been studied in some detail, well-defined, polymerization active

SSIPs are rare[15] and the kinetic and thermodynamic factors involved in the displacement of coordinated solvent by other solvent molecules or incoming monomers are poorly understood. The SSIPs, which have been studied,[16,17] have been probed mainly by computational methods and involve the most relevant Group 4 systems. Group 3 metal organocations are growing in importance,[18] and are also active polymerization catalysts, serving as excellent models for the behavior of this general class of early transition metal ion pairs.

It was within this context that we set out to explore the chemistry of some well-defined, base-free organoscandium dialkyl derivatives.[19] Organoscandium compounds supported by the bulky β-diketiminato ligands (Ar)NC(R)CHC(R)N(Ar) (Ar = 2,6-*i*Pr-C_6H_3; R = CH_3, L^{Me}; *t*Bu, L^{tBu}) of general formula $L^{R}ScR'_2$ (R′ = CH_3, CH_2CH_3, CH_2Ph, CH_2CMe_3, CH_2SiMe_3) have proven suitable for the study of cationic organoscandium compounds related to the organocations of Group 4 metals pertinent in olefin polymerization applications. For example, activation of dialkyls,[20] exemplified by $L^{tBu}ScMe_2$, with $B(C_6F_5)_3$ leads to CIPs whose dynamic behavior we have studied in detail.[21] Similar reactions with the dimethyl dimer incorporating the less sterically imposing L^{Me} ligand, $[L^{Me}ScMe_2]_2$, gave a CIP that rapidly neutralized via C_6F_5 transfer to the metal center.[21] However, activation of this complex with $[Ph_3C][B(C_6F_5)_4]$ in arene solvents gave remarkably stable solvent separated ion pairs (SSIPs) in which the methyl cation is stabilized by an arene solvent molecule bonded to the electrophilic metal center in a multihapto arrangement.[22] Here we describe these compounds in detail and the impact of coordinated arene on the insertion chemistry associated with the Sc-CH_3 moiety in the cation.

Results and Discussion

Synthesis and structure: Reaction of $[L^{Me}ScMe_2]_2$ with one equivalent of $[Ph_3C][B(C_6F_5)_4]$ in $[D_5]$bromobenzene leads to rapid and clean formation of a new compound, **1a**; its pattern for ligand resonances in the ^1H NMR spectrum is indicative of a symmetrical or fluxional species. The presence of an Sc-Me resonance at δ −0.10 ppm and characteristic peaks for the Ph_3CCH_3 by-product suggest formation of a cationic methyl species, but its observed thermal stability towards metalation contrasts with the facile loss of methane observed above −20 °C for the product of the analogous reaction between $L^{tBu}ScMe_2$ and $[Ph_3C][B(C_6F_5)_4]$ (Scheme 1). In this latter case, clean formation of $[L^{tBu}ScMe][B(C_6F_5)_4]$ (**2**), and Ph_3CCH_3 is observed at −30 °C, but upon warming, the symmetric pattern of ligand signals for **2** is supplanted by a more complex pattern consistent with metalation at the isopropyl methyl position.

While it is true that the organoscandium compounds supported by less sterically bulky L^{Me} are generally more resistant to metalation than those of L^{tBu},[19] this ligand effect is not significant enough to account for the marked increase in thermal stability of **1a** versus **2**. Fortunately, X-ray quality crystals of **1a** were obtained by layering the $[D_5]$bromobenzene solution with hexanes; the molecular structure determination revealed **1a** to be the SSIP $[L^{Me}Sc(\eta^6\text{-}C_6D_5Br)Me][B(C_6F_5)_4]$, in which a bromobenzene solvent molecule coordinates via the arene π system in an η^6-bonding mode. The presence of this coordinated solvent molecule apparently raises the barrier for metalation. While this solid state structure is not consistent with the observed symmetry of the molecule manifested in the ^1H NMR spectrum, the pattern can be explained by invoking a rapid exchange between coordinated and free $[D_5]$bromobenzene on the NMR timescale; bromobenzene cannot be cooled enough to freeze this process out.

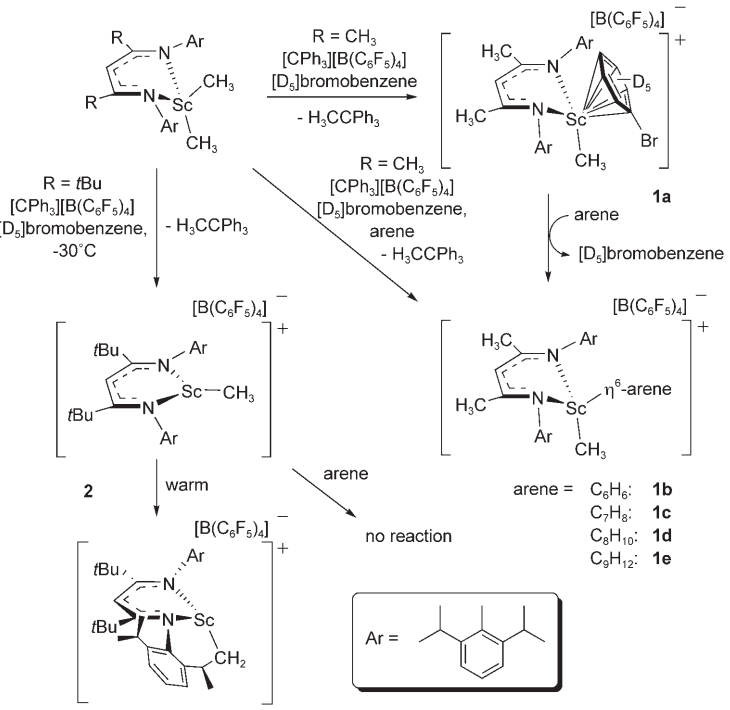

Scheme 1. Synthesis of scandium methyl SSIPs.

Spectral evidence for arene coordination in solution can be obtained, however, by treating **1a** with more electron rich arenes such as benzene (yielding **1b**), toluene (**1c**), *para*-xylene (**1d**) or mesitylene (**1e**) as shown in Scheme 1. Compounds **1b–e** can be generated directly via reaction of $[L^{Me}ScMe_2]_2$ and $[Ph_3C][B(C_6F_5)_4]$ in $[D_5]$bromobenzene in the presence of as little as one equivalent of the required arene. Coordination of the arene is indicated by upfield shifted resonances for the aromatic CH protons, and the manifestation of broken "top–bottom" symmetry in these formally C_s symmetric compounds. Specifically, four isopropyl methyl resonances and two isopropyl methine signals are observed in compounds **1b–e**, indicating that these structures are static on the NMR timescale; furthermore, signals for **1a** are completely absent in these spectra, despite being acquired in $[D_5]$bromobenzene; this indicates a strong preference for benzene/toluene/*p*-xylene/mesitylene binding over bromobenzene.

Table 1. Selected bond lengths [Å] and angles [°] for SSIPs **1a**, **1b**, and **1e**.

Parameter	**1a**	**1c**	**1e**
Sc–N1	2.100(4)	2.098(3)	2.120(4)
Sc–N2	2.105(4)	2.109(3)	2.097(4)
Sc–C1	2.162(5)	2.186(4)	2.212(4)
Sc–C32	2.842(4)	2.796(4)	2.773(5)
Sc–C33	2.767(4)	2.722(4)	2.795(5)
Sc–C34	2.682(4)	2.655(4)	2.843(5)
Sc–C35	2.640(4)	2.643(4)	2.736(5)
Sc–C36	2.715(4)	2.704(4)	2.701(5)
Sc–C37	2.802(5)	2.769(4)	2.694(5)
N1-Sc-N2	90.8(1)	90.5(1)	90.5(1)
C1-Sc-N1	105.2(2)	105.0(1)	102.7(2)
C1-Sc-N2	105.2(2)	104.5(1)	101.2(2)

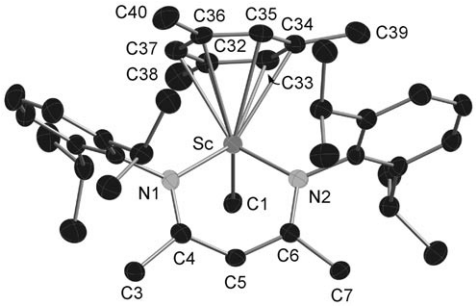

Figure 2. Thermal ellipsoid diagram (50%) of the cationic portion of η^6-**1e**. Selected metrical data is given in Table 1, while full details are given in the Supporting Information.

The molecular structures of toluene and mesitylene adducts **1c** and **1e** were confirmed by X-ray crystallography; ORTEP diagrams of each are given in Figures 1 and 2, respectively, while comparative metrical data for **1a**, **c** and **e** are provided in Table 1. Like all other organoscandium compounds incorporating these bulky β-diketiminato ligands, steric interactions between the *ortho*-isopropyl groups and the reactive ligands on scandium forces the metal out of the plane defined by the N_2C_3 ligand backbone in arene compounds **1**. We have defined the resulting diastereotopic coordination sites on scandium as the *exo* and *endo* positions, depending on their orientation relative to this ligand backbone plane. As can be seen in Figures 1 and 2, the arene ligands in **1c** and **e** occupy the *exo* site in the solid state. The NMR spectra discussed above suggest that this structure is maintained in solution, since exchanging diastereomers as a consequence of "ligand-flip" are not observed in these systems, in contrast to the CIPs formed upon activation with $B(C_6F_5)_3$.[21]

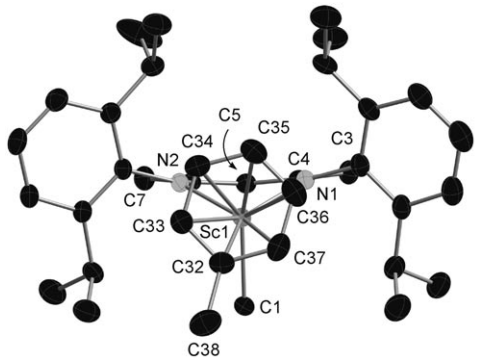

Figure 1. Thermal ellipsoid diagram (50%) of the cationic portion of η^6-**1c**. Selected metrical data is given in Table 1, while full details are given in the Supporting Information.

As in **1a**, the arene ligands in **1c** and **1e** can be regarded as η^6-bound, but the bonding to the arene carbons is not symmetrical. In **1c**, Sc–C_{arene} bond lengths ranging from 2.643(4)–2.796(4) Å are observed, causing significant tilting of the ring plane relative to the Sc-arene centroid vector. The analogous range in **1a** is 2.680(4)–2.842(4) Å, suggesting the larger Br substituents on the arene has a greater steric impact than the methyl group in toluene adduct **1c**. For **1e**, the range of Sc–C_{arene} distances 2.694(5)–2.843(5) Å is similar to that in **1c**. All of these distances agree well with those observed for a related CIP scandium cation featuring a coordinated $[\eta^6\text{-}C_6H_5CH_2)B(C_6F_5)_3]$ anion.[20]

No close contacts (< 4.9 Å) between the borate anion and the metal center were observed in any of the three structurally characterized compounds, solidifying their description as SSIP models. The preference for η^6-arene bonding is apparently quite strong in these species, since bromobenzene might be expected to bond in an η^1 fashion through the bromine atom.[23] The arene bonding is, however, quite sensitive to steric factors. Despite the greater basicity of mesitylene versus toluene,[24] toluene readily displaces mesitylene (see below). The greater steric tension within **1e** is evidenced by the greater degree of deviation from orthogonality observed for the *N*-aryl 2,6-diisopropyl phenyl substituents relative to the N_2C_3 ligand plane in **1e** versus **1c**. Furthermore, no evidence for any arene coordination, even for benzene, is observed when $[L^{tBu}ScMe][B(C_6F_5)_4]$ (**2**) is generated in the presence of these more basic arenes (Scheme 1); the *t*Bu groups of the ligand backbone push the N-aryl groups forward by 6–8°, such that η^6-arene binding is not feasible in the ground state, and rapid metalation ensues upon warming.

Arene exchange: Although the more basic arenes coordinate preferentially to the scandium center over bromobenzene, qualitative observations suggest that the coordinated solvent molecules are quite labile. For example, treatment of **1c** with an excess of $[D_8]$toluene results in a rapid loss of the signals for coordinated proteo toluene and production of one equivalent of free C_7H_8. Furthermore, treatment of **1c** with an excess of mesitylene, or **1e** with an excess of toluene, gives the other adduct quantitatively within the detection limits of NMR spectroscopy. Indeed, an equilibrium between **1c** and **e** is observed upon treatment of mesitylene adduct **1e** with one equivalent of toluene in bromobenzene (Table 2, Scheme 2); at 305 K the observed K_{eq} is 20.1(9). The temperature dependence of K_{eq} was evaluated over the

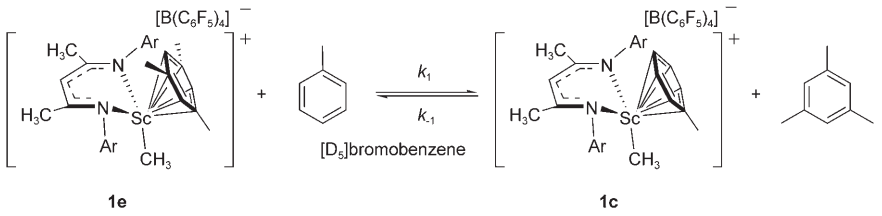

1e 1c

Scheme 2. Arene exchange equilibrium between **1e** and **c**.

Table 2. Kinetic data for the treatment of mesitylene adduct **1e** with one equivalent of toluene in bromobenzene (see Scheme 2).

T [K]	K_{eq}	$\Delta G^{\ddagger}$ [kcal mol^{-1}]
264(2)	12.3(7)	−1.3
289(2)	15.7(8)	−1.6
305(2)	20.1(9)	−1.8
324(2)	23.5(9)	−2.0

range 264–324 K and a van't Hoff analysis shows that ΔH° = 1.9(2) kcal mol^{-1} and ΔS° = 12(1) eu. Thus, the reaction preference for toluene binding is not large and is entropically driven, perhaps in part because of the enhanced conformational freedom enjoyed by the η^6-bound toluene molecule versus the more sterically locked η^6-mesitylene ligand. More significantly, at 65.38(1) eu,[25] free mesitylene has a larger molar entropy than toluene (52.4(3) eu).[26]

Although arene exchange is reversible, the rates of reaction in both directions of the equilibrium in Scheme 2 can be studied using pseudo first order kinetic techniques. Analysis of the forward reaction (k_1 in Scheme 2) in this way gave a pseudo first order rate constant of 2.16×10^{-2} s^{-1} at 298 K, and an Eyring analysis yielded $\Delta H^{\ddagger}$ of 21.4(6) kcal mol^{-1} and $\Delta S^{\ddagger}$ of 6(1) cal mol^{-1} K^{-1}, for $\Delta G^{\ddagger}$ of 19.5 kcal mol^{-1} at 298 K. Furthermore, at moderate concentrations of toluene (10–40 equivalents), k_{exp} exhibited no dependence on the [toluene] at 260 K; at higher [toluene] (50–200 equivalents), significant rate depression was observed, likely due to the impact of high [toluene] on the dielectric constant of the reaction medium. Taken together, these observations were interpreted in terms of a mechanism involving ring slippage of the η^6-mesitylene ligand to a lower (but undetermined) hapticity bonding mode as the rate limiting step, followed by rapid attack by toluene on the now more open metal to displace the mesitylene and form an η^n ($n < 6$) toluene adduct that collapses to the product **1c** (Scheme 3). The small but positive $\Delta S^{\ddagger}$ and the lack of dependence of k_{exp} on [toluene] are consistent with the dissociative character of the rate limiting step.

Interestingly, a similar set of experiments starting from toluene adduct **1c** and treating with high concentrations of mesitylene gave a pseudo first order rate constant k_{exp} of 0.15 s^{-1} at 298 K and activation parameters somewhat different in character than for the mesitylene displacement experiments discussed above. Eyring analysis gave $\Delta H^{\ddagger}$ = 17.5(3) kcal mol^{-1} and $\Delta S^{\ddagger}$ = −11(2) cal mol^{-1} K^{-1}, for $\Delta G^{\ddagger}$ = 20.5 kcal mol^{-1} at 298 K. Thus, $\Delta H^{\ddagger}$ is lower in this direction, consistent with the observed enthalpic preference for mesitylene in the ground state structures, while $\Delta S^{\ddagger}$ is now negative, suggesting a pathway that is associative in character in this direction. In

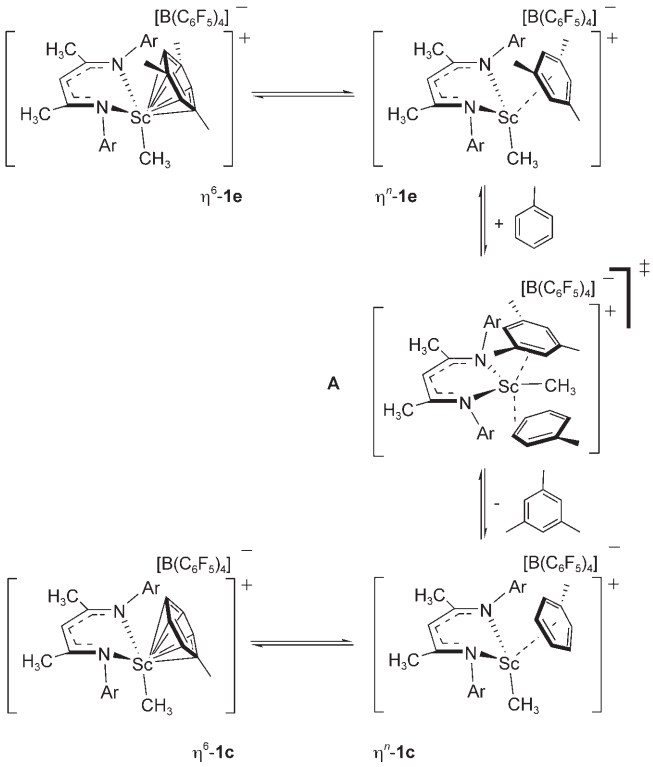

Scheme 3. Mechanism of arene exchange.

the context of the mechanistic proposal of Scheme 3, this implies that ring slippage of the enthalpically more weakly bound η^6-toluene ligand is no longer the rate limiting step in attaining the transition state **A** in Scheme 3; rather, the coordination of the bulky mesitylene arene has the higher barrier between ring slippage and arene association in this direction.[27]

Despite these nuances, overall, the character of the mechanism of displacement is identical in both directions, involving ring slippage to a lower coordinate, higher energy, species which then accepts the incoming arene to consummate the displacement. Most other mechanistic studies of arene exchange involve d^n metal systems,[28] and although the displacement of arene in these complexes generally have relatively high barriers, they are generally thought to proceed via lower hapticity intermediates as well. Interestingly, previously characterized arene complexes of cationic d^0 complexes with relevance to olefin polymerization appear to ex-

hibit a high barrier to arene exchange,[29] like their d^n counterparts. The facility with which compounds **1** undergo such exchange is a sign that the steric crowding about the metal center has reached a level that encourages ring slippage to the lower hapticity intermediates necessary to initiate the exchange process. The balance is, however, subtle. When **1e** is dissolved in [D_5]bromobenzene and exposed to 1 atm ethylene, polyethylene formation is immediate; when the same experiment is carried out in toluene, no polymer formation is observed. Toluene's stultifying effect on polymerization has been noted before,[4a] but evidently in the absence of a vast excess of strongly coordinating arene (toluene, mesitylene, etc.), ethylene is capable of displacing mesitylene to initiate polymerization.

Insertion of diphenylacetylene in 1e: The process by which arene is displaced in compounds **1** was studied further via stoichiometric reaction between **1e** and diphenylacetylene. This reaction proceeds smoothly at −30 °C to cleanly afford complex **3** (see Scheme 4), which arises via insertion of the

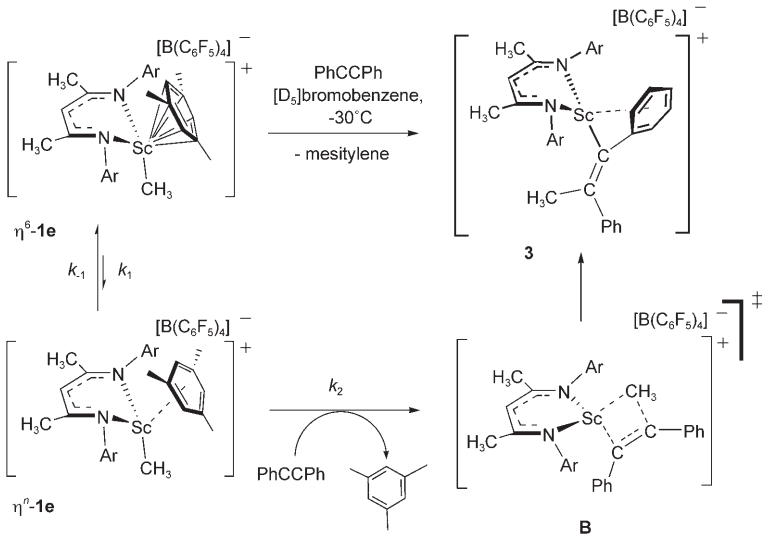

Scheme 4. Insertion of diphenylacetylene into **1e**.

alkyne into the Sc–Me bond. The progress of the reaction was conveniently followed by ^{1}H NMR spectroscopy as the Sc-Me resonance at δ −0.14 ppm was gradually replaced by a new signal at 1.40 ppm for the vinylic methyl resonance of **3**. Likewise, the ligand backbone CH resonances are baseline resolved with distinct peaks at δ 5.25 and 5.11 ppm for the **1e** starting material and **3**, respectively. While it proved difficult to grow single crystals of **3**, elemental analysis and multinuclear NMR spectroscopy supported the assignment; in particular, upfield shifted aromatic CH resonances for one of the phenyl rings (6.73, 6.38 and 6.22 ppm) suggest π interaction between this ring and the metal center as depicted. Given this intramolecular arene stabilization, one equivalent of free mesitylene is present in these reactions. Diagnostic resonances for the vinyl fragment are observed at 160.6 and 159.6 ppm in the ^{13}C{^{1}H} NMR spectrum and are more consistent with vinylic fragments which donate to the metal center[30] than those that do not.[31] On a preparative scale, **3** is isolable in 61 % yield as a somewhat tacky yellow solid.

The insertion reaction in Scheme 4 was conveniently monitored via ^{1}H NMR spectroscopy over the relatively narrow temperature range of 276–310 K in [D_5]bromobenzene under pseudo first order conditions (10–40 equivalents of diphenylacetylene). Integration of the ligand methine resonances provided the necessary concentration data, allowing for determination of pseudo first order rate constants under a variety of conditions (Table 3). As in the arene exchange experiments described above, the reaction was found to be first order in [**1e**] and evaluation of the rate at various temperatures followed by an Eyring treatment, afforded the activation parameters $\Delta H^{\ddagger} = 18.5(2)$ kcal mol^{-1} and $\Delta S^{\ddagger} = -17(2)$ eu[32] Thus, in contrast to the exchange of mesitylene for toluene, but in common with the reverse reaction, the insertion of diphenylacetylene via displacement of mesitylene appears to be characterized by a rate limiting substrate binding step, rather than rate limiting ring slippage of the mesitylene to the lower hapticity intermediate.

Accordingly, kinetic studies utilizing various equivalencies of diphenylacetylene substrate showed a marked dependence of k_{obs} on [PhCCPh] at 305 K (Figure 3, top), although there is some curvature in the plot indicating that at higher [PhCCPh], the onset of saturation behavior is occurring. These observations may be interpreted in terms of the mechanism shown in Scheme 4, wherein slippage to η^n-**1e** allows for rate limiting alkyne

Table 3. Pseudo first order rate constants in the reactions of diphenylacetylene with SSIPs **1**.

Entry	SSIP	[PhCCPh] [M]	T [K]	k_{obs} [s^{-1}]
1	**1e**	0.215	276	$7.20(7)\times10^{-6}$
2	**1e**	0.215	288	$3.26(4)\times10^{-5}$
3	**1e**	0.215	300	$2.30(8)\times10^{-4}$
4	**1e**	0.215	305	$2.51(2)\times10^{-4}$
5	**1e**[a]	0.215	310	$4.54(7)\times10^{-4}$
6	**1e**	0.430	305	$6.70(6)\times10^{-4}$
7	**1e**	0.645	305	$9.25(8)\times10^{-4}$
8	**1e**	0.860	305	$1.12(1)\times10^{-3}$
9	**1a**	0.215	300	$1.36(5)\times10^{-3}$
10	**1b**	0.215	300	$2.00(6)\times10^{-4}$
11	**1c**	0.215	300	$1.30(3)\times10^{-4}$

[a] Average of four separate runs.

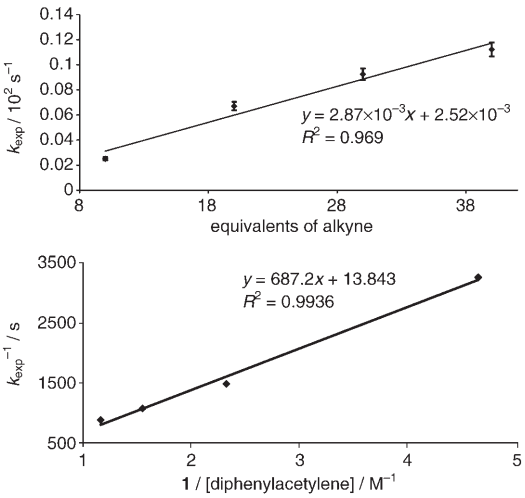

Figure 3. Top) Plot of k_{obs} versus [PhCCPh] in the reaction of η^6-**1e** with diphenylacetylene. Bottom) Double reciprocal plot of $1/k_{obs}$ versus 1/[PhCCPh] in the reaction of η^6-**1e** with diphenylacetylene.

binding followed by insertion via the familiar four-center transition state **B**. (While it is conceivable that an η^n-PhCCPh complex binding through one of the phenyl rings of the alkyne lies on the reaction coordinate, we found no evidence for such an intermediate by low temperature NMR spectroscopy.) Alkyne binding is often rate limiting in alkyne insertion reactions involving d^0 complexes.[33,34] Assuming that [η^n-**1e**] is present in a steady state, one can arrive at the rate law shown in Equation (1):

$$\text{rate} = k_{obs}[\eta^6\text{-}\mathbf{1e}]$$

$$k_{obs} = k_1k_2[\text{PhCCPh}]/k_{-1} + k_2[\text{PhCCPh}] \quad (1)$$

Thus a double reciprocal plot (Figure 3, bottom) of $1/k_{obs}$ versus 1/[PhCCPh] yields an intercept equal to $1/k_1$ and a slope equal to k_{-1}/k_1k_2. From this treatment, values for k_1 of 0.072 s^{-1} and for k_{-1}/k_2 of 43 are obtained. The former compares to a value of 0.057 s^{-1} at 305 K, calculated from a $\Delta G^{\ddagger}$ of 19.6 kcal mol^{-1} measured in the arene exchange experiments described above, a barrier assigned to the rate of ring slippage from η^6 to η^n binding, that is, k_1 in Scheme 4. This provides corroborative evidence that the first steps in both reactions are the same, and involve the ring slippage process proposed. The ratio of k_{-1} to k_2 is small enough that at higher [PhCCPh], the k_2[PhCCPh] term in the rate law begins to compete with k_{-1} and saturation behavior is observed. Unfortunately, it was practically difficult to go beyond 40 equivalents of alkyne to provide more solid evidence for this scenario.

The impact of arene binding to these methyl cations on the rate of insertion of an alkyne, which serves as a model for the propagation step in olefin enchainment processes, is clear from these experiments. Much of the barrier to this insertion process is comprised of the energy required to access lower hapticity arene intermediates. Accordingly, k_{obs} for alkyne insertion varies with the nature of the arene present, with faster reactions observed for more weakly binding arenes (Table 3, entries 3, 9–11) Furthermore, when arene is not present, as in methyl cation **2**, insertion of diphenylacetylene is immeasurably fast using the NMR methods employed here, even at temperatures below −20 °C. Since arene binding was not detected in this system, either there is no interaction between the solvent and the metal center, or that which is present is of low hapticity,[35] and therefore very weak, allowing for unimpeded substrate binding and insertion in the system, even though the actual ancillary ligand is more sterically bulky than the methyl substituted derivatives in compounds **1**.

Conclusion

In summary, a unique family of isolable solvent separated organoscandium methyl cations have been synthesized. These complexes are supported by a sterically bulky β-diketiminato ligand and have been found to be resistant to both C_6F_5 transfer and metalation decomposition pathways. Their solution and solid-state structures have been explored using multinuclear NMR and X-ray crystallography. Quantitative kinetic experiments for arene exchange from **1e** to **c** imply a partially dissociative mechanism whereby the rate limiting step involves dissociation to lower hapticity. The mechanism for arene displacement was further investigated upon exploring the reactivity of these SSIPs with diphenylacetylene where it was determined that rate limiting coordination of the alkyne to the metal centre had a slightly higher barrier than arene ring slipping.

Experimental Section

General considerations: An argon filled Innovative Technology System One glove box was employed for manipulation and storage of all oxygen and moisture sensitive compounds. All reactions were performed on a double manifold high vacuum line using standard techniques.[36] Residual oxygen and moisture were removed from the argon stream by passage through an OxisorBW scrubber from Matheson Gas Products. Toluene, hexanes, and tetrahydrofuran (THF) solvents were dried and purified using the Grubbs/Dow purification system[37] and stored in evacuated 500 mL bombs over titanocene[38] (toluene and hexanes) or sodium/benzophenone (THF). Benzene, [D_6]benzene, [D_8]toluene, [D_8]THF and hexmethyldisiloxane were dried and stored over sodium/benzophenone in glass bombs under vacuum. NMR spectroscopy (^{1}H, ^{2}H, ^{11}B, ^{13}C{^{1}H}, ^{19}F, DEPT-135, DEPT-90, HMQC, EXSY,[39] ROESY and COSY experiments) was performed on Bruker AC-200 (^{1}H 200.134 MHz, ^{13}C{^{1}H} 50.323 MHz), Bruker AMX-300 (^{1}H 300.138 MHz, ^{2}H 46.073 MHz, ^{11}B{^{1}H} and ^{11}B 96.293 MHz, ^{13}C{^{1}H} 75.478 MHz, ^{19}F 282.371 MHz) or Bruker DRX-400 (^{1}H 400.134 MHz, ^{13}C{^{1}H} 100.614 MHz, ^{11}B 128.375 MHz) spectrometers. All 2D NMR experiments were performed using Bruker AMX-300 or Bruker-DRX 400 spectrometers. All ^{1}H NMR spectra were referenced to $SiMe_4$ through the residual ^{1}H resonance(s) of the employed solvent; [D_6]benzene (7.16 ppm), [D_8]toluene (2.09, 6.98, 7.02 and 7.09 ppm) or [D_5]bromobenzene (6.94, 7.02 and 7.30 ppm). ^{2}H NMR spectra were referenced relative to an external standard of [D_{12}]TMS (0.0 ppm) prior to spectrum acquisition. ^{11}B NMR spectra were

referenced to an external standard of $BF_3{\cdot}Et_2O$ (0.0 ppm) prior to acquisition of the first spectrum. ^{13}C NMR spectra were referenced relative to $SiMe_4$ through the resonance(s) of the employed solvent; [D_6]benzene (128.0 ppm), [D_8]toluene (20.4, 125.2, 128.0, 128.9, 137.5 ppm) or [D_5]bromobenzene (122.3, 126.1, 129.3, 130.9 ppm). ^{19}F NMR spectra are referenced to $CFCl_3$ using an external standard of hexafluorobenzene (−163.0 ppm)[40] in [D_6]benzene prior to acquisition of the first spectrum. Temperature calibration for NMR experiments was achieved by monitoring the ^1H NMR spectrum of pure methanol (below room temperature) and pure ethylene glycol (above room temperature).[41] Elemental analyses were performed on a Control Equipment Corporation 440 Elemental Analyzer by Mrs. Dorothy Fox and Mrs. Roxanna Smith of this department. X-ray crystallographic analyses were performed on suitable crystals coated in Paratone 8277 oil (Exxon) and mounted on a glass fibre. Measurements were collected on a Nonius KappaCCD diffractometer by Dr. Masood Parvez of this department; full details can be found in the individual tables for each crystal structure (see Supporting Information). HL (L = ArNC(R)CHC(R)NAr where Ar = 2,6-*i*Pr-C_6H_3 and R = Me and *t*Bu),[42] $ScCl_3(THF)_3$[43] and the scandium dialkyls[19] were prepared by literature procedures. Scandium oxide (Sc_2O_3) was purchased from Boulder Scientific Co. and used as received. All deuterated solvents for NMR experiments were purchased from Cambridge Isotopes. All other reagents were purchased from Aldrich Chemicals and used as received.

Synthesis of η⁶–1a: A 25 mL round-bottom flask was charged with [$L^{Me}ScMe_2]_2$ (0.035 g, 0.072 mmol) and [CPh_3][$B(C_6F_5)_4$] (0.066 g, 0.072 mmol) to which bromobenzene (3 mL) was added. The solution was stirred for 5 min and then layered with hexanes (5 mL). The reaction mixture was cooled to −35 °C for 24 h and solvent decanted. The yellow crystals were washed with toluene (2×2 mL) and dried under vacuum to yield η⁶-**1a** as a fine yellow powder (0.067 g, 0.052 mmol, 72 %). ^1H NMR ([D_5]bromobenzene): δ = 7.24–7.02 (m, 6H; C_6H_3), 5.30 (s, 1H; CH), 2.35 (sp, 4H; C*H*Me_2, $J_{H,H}$ = 6.6 Hz), 1.59 (s, 6H; NCMe), 1.14 (d, 12H; CH*Me*$_2$, $J_{H,H}$ = 6.6 Hz), 0.88 (d, 12H; CH*Me*$_2$, $J_{H,H}$ = 6.6 Hz), −0.10 ppm (s, 3H; ScMe); $^{13}C\{^1H\}$ NMR ([D_5]bromobenzene, 270 K, C_6F_5 resonances not reported): δ = 170.3 (N*C*Me), 141.1 (C_{ipso}), 139.8, 128.5, 127.7 (C_6H_3), 97.6 (CH), 45.3 (ScMe), 28.4 (*C*HMe_2), 24.0 (NC*Me*), 24.0, 23.7 ppm (CH*Me*$_2$); ^{19}F NMR ([D_5]bromobenzene): δ = −132.9(*o*-F), −163.0 (*p*-*F*), −166.9 ppm (*m*-*F*); $^{11}B\{^1H\}$ NMR ([D_5]bromobenzene): δ = −17.0 ppm; elemental analysis calcd (%) for $C_{60}H_{49}N_2BF_{20}BrSc$: C 54.86, H 3.76, N 2.13; found: C 54.24, H 3.80, N 1.98.

Synthesis of η⁶-1b: A 25 mL round-bottom flask was charged with [$L^{Me}ScMe_2]_2$ (0.035 g, 0.072 mmol) and [CPh_3][$B(C_6F_5)_4$] (0.066 g, 0.072 mmol) to which bromobenzene (3 mL) was added. The solution was stirred for 5 min during which period benzene (2 mL) was added dropwise. The reaction mixture was layered with hexanes (5 mL), cooled to −35 °C for 24 h and solvent decanted. The yellow crystals were washed with toluene (2×2 mL) and dried under vacuum to give η⁶-**1b** as a fine yellow powder (0.054 g, 0.044 mmol, 62 %). ^1H NMR ([D_5]bromobenzene, 270 K): δ = 7.22–7.10 (m, 6H; C_6H_3), 6.85 (s, 6H; C_6H_6), 5.21 (s, 1H; CH), 2.46 (sp, 2H; C*H*Me_2, $J_{H,H}$ = 6.8 Hz), 2.18 (sp, 2H; C*H*Me_2, $J_{H,H}$ = 6.8 Hz), 1.55 (s, 6H; NCMe), 1.19 (d, 6H; CH*Me*)$_2$, $J_{H,H}$ = 6.8 Hz), 1.11 (d, 6H; CH*Me*$_2$, $J_{H,H}$ = 6.8 Hz), 1.01 (d, 6H; CH*Me*$_2$, $J_{H,H}$ = 6.8 Hz), 0.73 (d, 6H; CH*Me*$_2$, $J_{H,H}$ = 6.8 Hz), −0.28 ppm (s, 3H; ScMe); $^{13}C\{^1H\}$ NMR ([D_5]bromobenzene, 270 K, C_6F_5 resonances not reported): δ = 169.7 (N*C*Me), 142.4 (C_{ipso}), 140.7, 139.8 (C_6H_3), 132.2 (C_6H_6), 129.9, 127.9, 124.7 (C_6H_3), 96.9 (CH), 41.5 (ScMe), 28.4, 27.5 (*C*HMe_2), 24.3, 23.9 (CH*Me*$_2$), 23.8 (NC*Me*), 23.7, 22.4 ppm (CH*Me*$_2$); ^{19}F NMR ([D_5]bromobenzene, 250 K): δ = −131.1 (*o*-*F*), −161.0 (*p*-*F*), −164.9 ppm (*m*-*F*); $^{11}B\{^1H\}$ NMR ([D_5]bromobenzene, 250 K): δ = −17.0 ppm; elemental analysis calcd (%) for $C_{60}H_{50}N_2BF_{20}Sc{\cdot}C_6H_5Br$: C 56.96, H 3.98, N 2.01; found: C 54.26, H 3.71, N 1.86. Repeated attempts consistently gave low carbon analyses, despite recrystallization of the sample. This poor combustion may be due to formation of scandium nitrides or carbides.

Synthesis of η⁶-1c: A 25 mL round-bottom flask was charged with [$L^{Me}ScMe_2]_2$ (0.035 g, 0.072 mmol) and [CPh_3][$B(C_6F_5)_4$] (0.066 g, 0.072 mmol) to which bromobenzene (3 mL) was added. The solution was stirred for 5 min, toluene (2 mL) was added followed by an additional 5 min of stirring. The reaction mixture was layered with hexanes (5 mL), cooled to −35 °C for 24 h and solvent decanted. The yellow solid was washed with toluene (2×2 mL) and dried under vacuum to give η⁶-**1c** as a bright yellow powder (0.087 g, 0.071 mmol, 98 %). ^1H NMR ([D_5]bromobenzene, 260 K): δ = 7.22–7.10 (m, 6H; C_6H_3), 6.81 (d, 2H; *o*-C_7H_8, $J_{H,H}$ = 7.5 Hz), 6.66 (t, 1H; *p*-C_7H_8, $J_{H,H}$ = 7.5 Hz), 6.39 (t, 2H; *m*-C_7H_8, $J_{H,H}$ = 7.5 Hz), 5.18 (s, 1H; CH), 2.44 (sp, 2H; C*H*Me_2, $J_{H,H}$ = 6.7 Hz), 2.19 (sp, 2H; C*H*Me_2, $J_{H,H}$ = 6.7 Hz), 1.86 (s, 3H; *Me*Ph), 1.50 (s, 6H; NCMe), 1.16 (d, 6H; CH*Me*$_2$, $J_{H,H}$ = 6.7 Hz), 1.06 (d, 6H; CH*Me*$_2$, $J_{H,H}$ = 6.7 Hz), 1.01 (d, 6H; CH*Me*$_2$, $J_{H,H}$ = 6.7 Hz), 0.72 (d, 6H; CH*Me*$_2$, $J_{H,H}$ = 6.7 Hz), −0.29 ppm (s, 3H; ScMe); $^{13}C\{^1H\}$ NMR ([D_5]bromobenzene, 270 K, C_6F_5 resonances not reported): δ = 169.8 (N*C*Me), 142.3 (C_{ipso} of C_6H_3), 140.7, 139.9 (C_6H_3), 137.3 (C_{ipso} of MePh), 133.2, 132.7 (Me*Ph*), 128.3, 127.7 (C_6H_3), 126.0 (Me*Ph*), 125.5 (C_6H_3), 97.6 (CH), 42.7 (ScMe), 28.8, 27.8 (*C*HMe_2), 24.7 (CH*Me*$_2$), 24.1 (NC*Me*), 24.1, 24.0, 22.6 ppm (CH*Me*$_2$), 21.3 (Ph*Me*); ^{19}F NMR ([D_5]bromobenzene, 250 K): δ = −131.2 (*o*-*F*), −161.0 (*p*-*F*), −164.9 ppm (*m*-*F*); ^{11}B NMR ([D_5]bromobenzene, 250 K): δ = −17.0 ppm; elemental analysis calcd (%) for $C_{61}H_{52}N_2BF_{20}Sc{\cdot}C_6H_5Br$: C 57.24, H 4.09, N 1.99; found: C 56.94, H 3.87, N 2.39.

Synthesis of η⁶-1d: A 25 mL round-bottom flask was charged with [$L^{Me}ScMe_2]_2$ (0.023 g, 0.047 mmol) and [CPh_3][$B(C_6F_5)_4$] (0.043 g, 0.047 mmol) to which bromobenzene (3 mL) was added. The solution was stirred for 5 minutes, *p*-xylene (2 mL) was added followed by an additional 5 min of stirring. The reaction mixture was layered with hexanes (5 mL), cooled to −35 °C for 36 h and solvent decanted. The oily yellow solid was washed with toluene (2×2 mL) and dried under vacuum to give η⁶-**1d** as a yellow powder (0.030 g, 51 %). ^1H NMR ([D_5]bromobenzene, 250 K): δ = 7.22–6.97 (m, 6H; C_6H_3), 6.65 (s, 4H; 1,4-Me-C_6H_4), 5.24 (s, 1H; CH), 2.35 (sp, 2H; C*H*Me_2, $J_{H,H}$ = 6.6 Hz), 2.12 (sp, 2H; C*H*Me_2, $J_{H,H}$ = 6.6 Hz), 1.58 (s, 6H; 1,4-*Me*-C_6H_4), 1.48 (s, 6H; NCMe), 1.14 (d, 12H; CH*Me*$_2$, $J_{H,H}$ = 6.6 Hz), 0.97 (d, 6H; CH*Me*$_2$, $J_{H,H}$ = 6.6 Hz), 0.70 (d, 6H; CH*Me*$_2$, $J_{H,H}$ = 6.6 Hz), −0.30 ppm (s, 3H; ScMe); $^{13}C\{^1H\}$ NMR ([D_5]bromobenzene, 250 K, C_6F_5 resonances not reported): δ = 169.7 (N*C*Me), 143.4 (C_{ipso} of C_6H_3), 141.6, 140.1 (C_6H_3), 132.9 (C_{ipso} of 1,4-Me-C_6H_3), 129.0 (1,4-Me-C_6H_3), 128.7, 127.9, 127.8 (C_6H_3), 97.6 (CH), 42.3 (ScMe), 30.4, 28.7 (*C*HMe_2), 24.6 (NC*Me*), 24.3, 24.2, 24.1, 22.8 (CH*Me*$_2$), 20.4 ppm (1,4-*Me*-C_6H_3); ^{19}F NMR ([D_5]bromobenzene, 250 K): δ = −131.2 (*o*-*F*), −161.0 (*p*-*F*), −164.9 ppm (*m*-*F*); ^{11}B NMR ([D_5]bromobenzene, 250 K): δ = −16.7 ppm; elemental analysis calcd (%) for $C_{62}H_{54}N_2BF_{20}Sc{\cdot}C_6H_5Br$: C 57.52, H 4.19, N 1.97; found: C 54.70, H 3.81, N 1.58. Repeated attempts consistently gave low carbon analyses, despite recrystallization of the sample. This poor combustion may be due to formation of scandium nitrides or carbides.

Synthesis of η⁶-1e: A 25 mL round-bottom flask was charged with [$L^{Me}ScMe_2]_2$ (0.045 g, 0.091 mmol) and [CPh_3][$B(C_6F_5)_4$] (0.084 g, 0.091 mmol) to which bromobenzene (5 mL) was added. The solution was stirred for 5 min, mesitylene (1 mL) was added followed by an additional 5 min of stirring. The reaction mixture was layered with hexanes (5 mL), cooled to −35 °C for 18 h and solvent decanted. The large yellow crystals were washed with toluene (3×2 mL) and dried under vacuum to give η⁶-**1e** as a yellow powder (0.110 g, 0.088 mmol, 97 %). ^1H NMR ([D_5]bromobenzene, 250 K): δ = 7.26–6.88 (m, 6H; C_6H_3), 6.59 (s, 3H; 1,3,5-Me-C_6H_3), 5.25 (s, 1H; CH), 2.37 (sp, 2H; C*H*Me_2, $J_{H,H}$ = 6.6 Hz), 2.09 (sp, 2H; C*H*Me_2, $J_{H,H}$ = 6.6 Hz), 1.43 (s, 6H; NCMe), 1.36 (s, 9H; 1,3,5-*Me*-C_6H_3), 1.17 (d, 6H; CH*Me*$_2$, $J_{H,H}$ = 6.6 Hz), 1.08 (d, 6H; CH*Me*$_2$, $J_{H,H}$ = 6.6 Hz), 0.95 (d, 6H; CH*Me*$_2$, $J_{H,H}$ = 6.6 Hz), 0.74 (d, 6H; CH*Me*$_2$, $J_{H,H}$ = 6.6 Hz), −0.14 ppm (s, 3H; ScMe); $^{13}C\{^1H\}$ NMR [D_5]bromobenzene, 250 K, C_6F_5 resonances not reported): δ = 170.4 (N*C*Me), 141.7 (C_{ipso} of C_6H_3), 141.2, 140.8 (C_6H_3), 137.2 (C_{ipso} of 1,3,5-Me-C_6H_3), 130.0 (1,3,5-Me-C_6H_3), 127.0, 126.8, 124.9 (C_6H_3), 98.8 (CH), 43.5 (ScMe), 29.1, 28.3 (*C*HMe_2), 24.8 (NC*Me*), 24.6, 24.1, 23.5, 23.1 (CH*Me*$_2$), 21.4 ppm (1,3,5-*Me*-C_6H_3); ^{19}F NMR ([D_5]bromobenzene, 250 K): δ = −131.2 (*o*-*F*), −161.1 (*p*-*F*), −165.0 ppm; ^{11}B NMR ([D_5]bromobenzene, 250 K): δ −16.6 ppm; elemental analysis calcd (%) for $C_{63}H_{56}N_2BF_{20}Sc$: C 59.26, H 4.42, N 2.19; found: C 58.75, H 4.34, N 2.21.

In situ generation of 2: An NMR tube was charged with $L^{tBu}ScMe_2$ (0.010 g, 0.017 mmol) and $[Ph_3C][B(C_6F_5)_4]$ (0.016 g, 0.017 mmol). The tube was cooled to −30 °C, cold (−30 °C) [D_5]bromobenzene (0.5 mL) was added and the sample was slowly allowed to warm to 285 K. ^{1}H NMR (285 K, [D_5]bromobenzene): δ = 7.11–6.97 (m, 6H; C_6H_3), 5.95 (s, 1H; CH), 2.46 (sp, 4H; C*H*Me_2, $J_{H,H}$ = 6.8 Hz), 1.12 (d, 12H; CH*Me*$_2$, $J_{H,H}$ = 6.8 Hz), 1.02 (s, 18H; NCC*Me*$_3$), 0.82 (d, 12H; CH*Me*$_2$, $J_{H,H}$ = 6.8 Hz), −0.12 ppm (s, 3H; ScMe); ^{13}C{^{1}H} NMR ([D_5]bromobenzene, C_6F_5 resonances not reported): δ = 174.5 (N*C*CMe$_3$), 140.0 (C_{ipso}), 138.8, 128.3, 124.8 (C_6H_3), 91.8 (CH), 44.5 (*C*Me$_3$), 41.1 (ScMe), 30.9 (C*Me*$_3$), 29.7 (*C*HMe$_2$), 25.7, 22.9 ppm (CH*Me*$_2$); ^{19}F NMR ([D_5]bromobenzene): δ = −133.2 (*o*-*F*), −162.4 (*p*-*F*), −166.3 ppm (*m*-*F*); ^{11}B{^{1}H} NMR ([D_5]bromobenzene): δ = −17.0 ppm.

In situ generation of [{ArNC(*t*Bu)CHC(*t*Bu) NAr}Sc(PhC≡CMePh)][B(C$_6$F$_5$)$_4$]: Cold (−35 °C) [D_5]bromobenzene (0.4 mL) was added to an NMR tube charged with $L^{tBu}ScMe_2$ (0.015 g, 0.026 mmol) and $[CPh_3][B(C_6F_5)_4]$ (0.024 g, 0.026 mmol). Upon mixing of reagents a cold (−35 °C) [D_5]bromobenzene (0.3 mL) solution of diphenylacetylene (0.005 g, 0.028 mmol) was added dropwise. The tube was shaken and inserted into the NMR probe at −35 °C. ^{1}H NMR ([D_5]bromobenzene, 280 K): δ = 7.12–6.83 (m, 16H; Ph, C_6H_3), 5.69 (s, 1H; CH), 2.31 (br, 4H; C*H*Me_2), 1.71 (s, 3H; ScC≡CMe), 1.08–0.95 (m, 24H; CHMe_2), 0.89 ppm (s, 18H; NCCMe_3); ^{19}F NMR ([D_5]bromobenzene): δ = −132.8 (*o*-F), −163.2 (*p*-F), −167.0 ppm (*m*-F); ^{11}B{^{1}H} NMR ([D_5]bromobenzene): δ = −16.8 ppm. The instability of the compound made it impossible to acquire ^{13}C NMR spectra as further decomposition occurs over the timeframe required to collect the necessary data.

Synthesis of 3: Bromobenzene (3 mL) was condensed into an evacuated flask containing η^6-**1e** (0.118 g, 0.0900 mmol) and diphenylacetylene (0.0160 g, 0.0900 mmol) at −35 °C. The yellow solution was gradually warmed to room temperature and allowed to stir for 2 d. Removal of solvent under vacuum gave a yellow/orange oil. Hexanes (5 mL) was added and the reaction mixture sonicated (5 min), filtered, and solvent removed to afford **3** as a fine yellow solid (0.081 g, 0.055 mmol, 61 %). ^{1}H NMR ([D_5]bromobenzene): δ = 7.56 (d, 2H; Ph, $J_{H,H}$ = 7.4 Hz), 7.49–6.96 (m, 8H; Ph), 6.80 (t, 1H; Ph, $J_{H,H}$ = 7.4 Hz), 6.73 (t, 1H; Ph, $J_{H,H}$ = 7.7 Hz), 6.38 (d, 2H; Ph, $J_{H,H}$ = 7.7 Hz), 6.22 (t, 2H; Ph, $J_{H,H}$ = 7.7 Hz), 5.25 (s, 1H; CH), 2.46 (sp, 2H; C*H*Me_2, $J_{H,H}$ = 6.7 Hz), 2.08 (sp, 2H; C*H*Me_2, $J_{H,H}$ = 6.7 Hz), 1.52 (s, 3H; ScC≡CMe), 1.45 (s, 6H; NCMe), 1.33 (d, 6H; CH*Me*$_2$, $J_{H,H}$ = 6.7 Hz), 1.09 (d, 6H; CH*Me*$_2$, $J_{H,H}$ = 6.7 Hz), 0.94 (d, 6H; CH*Me*$_2$, $J_{H,H}$ = 6.7 Hz), 0.73 ppm (d, 6H; CH*Me*$_2$, $J_{H,H}$ = 6.7 Hz); ^{13}C{^{1}H} NMR ([D_5]bromobenzene): δ = 169.4 (N*C*Me), 160.6 (ScC≡C), 159.6 (ScC≡C), 143.5, 142.8, 142.3, 141.5, 139.9, 136.9, 133.2, 131.3, 129.8, 126.9, 126.6, 125.0, 124.8, 123.3 (C_6H_3, Ph), 96.8 (CH), 28.6, 28.4 (*C*HMe$_2$), 25.3 (CH*Me*$_2$), 25.1 (NC*Me*), 24.3, 24.2, 23.4 (CH*Me*$_2$), 23.0 ppm (ScC≡C*Me*); ^{19}F NMR ([D_5]bromobenzene): δ = −132.9 (*o*-*F*), −163.1 (*p*-*F*), −167.0 ppm (*m*-*F*); ^{11}B{^{1}H} NMR ([D_5]bromobenzene): δ = −16.9 ppm; elemental analysis calcd (%) for $ScN_2BF_{20}C_{68}H_{54}$: C 61.18, H 4.08, N 2.10; found: C 60.82, H 4.58, N 1.85.

Error analysis: For all kinetic experiments estimated error values are depicted in brackets after the rate. These values were established upon judicious choice of potential sources of experimental error including temperature accuracy, integration accuracy, mass and concentration accuracy, NMR sensitivity, and sample purity. Each of these parameters was manually calculated for maximum error and the resultant effect that had on the measurement and any subsequent calculations. The summation of all such errors generated the total estimated error in brackets. This method is beneficial over routine standard deviation calculations in that it allows the calculation of potential systematic sources of error, such as temperature calibration of the NMR probe. In such circumstances it is possible to have high precision with low accuracy, and thus have a deceivingly low standard deviation. Before starting a kinetic experiment the T_1 of all relevant atoms was determined. A delay of at least five times the longest T_1 value was used in each kinetic experiment.

Kinetics of arene exchange in η^6-1c: In a typical experiment, η^6-**1c** (0.015 g, 0.0119 mmol, 2.14×10^{-2} M) was dissolved in [D_5]bromobenzene (0.53 mL), cooled to −35 °C, and cold mesitylene (0.020 mL, 0.147 mmol) was added. The NMR tube was kept at −35 °C until inserted into the probe, at which time it was given 10 min to equilibrate to the specified temperature. The progress of reaction was monitored by integration of the backbone peak in the ^{1}H NMR spectrum. The reaction was followed until 95 % completion.

Kinetics of arene exchange in η^6-1e: In a typical experiment, η^6-**1e** (0.015 g, 0.0118 mmol, 2.14×10^{-2} M) was dissolved in [D_5]bromobenzene (0.54 mL), cooled to −35 °C and cold toluene (0.012 mL, 0.0118 mmol) added. In the [toluene] dependence studies, this amount was varied. The NMR tube was kept at −35 °C until inserted into the NMR probe, at which time it was given 10 min to equilibrate to the specified temperature. The progress of reaction was monitored by integration of the backbone peak in the ^{1}H NMR spectrum. The reaction was followed until 95 % completion.

Equilibrium between η^6-1e and η^6-1c: In a typical experiment, η^6-**1e** (0.015 g, 0.012 mmol, 2.14×10^{-2} M) was dissolved in 0.54 mL [D_5]bromobenzene, cooled to −35 °C and 1 equivalent of cold toluene (1.2 μL, 0.012 mmol) was added. The NMR tube was kept at −35 °C until inserted into the NMR probe, at which time it was given 120 min to equilibrate to each temperature. K_{eq} was calculated from concentrations determined by integrations of the ligand backbone peak in the ^{1}H NMR spectrum. In order to ensure equilibrium had been achieved at a given temperature, a series of ^{1}H NMR spectra were recorded until identical results were obtained in three consecutive experiments.

Kinetics of the reaction of η^6–1e with PhCCPh: In a typical experiment, η^6–**1e** (0.015 g, 0.0118 mmol) was dissolved in [D_5]bromobenzene (0.3 mL), cooled to −35 °C and a [D_5]bromobenzene solution (0.3 mL) of diphenylacetylene (0.022 g, 0.118 mmol) was added. In the [PhCCPh] dependence studies, this amount was varied. The NMR tube was kept at −35 °C until inserted into the NMR probe, at which time it was given 10 min to equilibrate to the specified temperature. The progress of reaction was monitored by integration of the ligand backbone peak in the ^{1}H NMR spectrum. The reaction was followed until 95 % completion.

X-ray crystallography: X-ray crystallographic analyses were performed on suitable crystals coated in Paratone oil and mounted on a Nonius Kappa CCD diffractometer.

CCDC-213157 (η^6-**1c**) and -615768 (η^6-**1e**) contains the supplementary crystallographic data for this paper. These data can be obtained free of charge from The Cambridge Crystallographic Data Centre via www.ccdc.cam.ac.uk/data_request/cif.

Acknowledgements

Financial Support for this work was provided by NSERC of Canada in the form of a Discovery Grant to W.E.P. (2001–2003) and scholarship support to P.G.H. (PGS-A and PGS-B). P.G.H. also thanks the Alberta Heritage Foundation for a Steinhauer Award and the Sir Izaak Walton Killam Foundation for a Doctoral Fellowship. The authors thank Nova Chemicals Ltd., Calgary, Alberta, for a generous gift of $[CPh_3][B(C_6F_5)_4]$.

[1] a) R. F. Jordan, *Adv. Organomet. Chem.* **1991**, *32*, 325–387; b) M. Bochmann, *J. Chem. Soc. Dalton Trans.* **1996**, 255–270; c) M. Bochmann, *Top. Catal.* **1999**, *7*, 9–22; d) S. Arndt, J. Okuda, *Adv. Synth. Catal.* **2005**, *347*, 339–354; e) P. M. Zeimentz, S. Arndt, B. R. Elvidge, J. Okuda, *Chem. Rev.* **2006**, *106*, 2404–2433.

[2] E. Y. X. Chen, T. J. Marks, *Chem. Rev.* **2000**, *100*, 1391–1434.

[3] V. C. Gibson, S. K. Spitzmesser, *Chem. Rev.* **2003**, *103*, 283–315.

[4] a) J. D. Scollard, D. H. McConville, *J. Am. Chem. Soc.* **1996**, *118*, 10008–10009; b) J. D. Scollard, D. H. McConville, N. C. Payne, J. J. Vittal, *Macromolecules* **1996**, *29*, 5241–5243.

[5] J. D. Scollard, D. H. McConville, *Organometallics* **1997**, *16*, 1810–1812.

[6] W. E. Piers, *Adv. Organomet. Chem.* **2005**, *52*, 1–77.

[7] E. J. Stoebenau III, R. F. Jordan, *J. Am. Chem. Soc.* **2006**, *128*, 8638–8650.

[8] a) X. Yang, C. L. Stern, T. J. Marks, *Organometallics* **1991**, *10*, 840–842; b) G. G. Hlatky, D. J. Upton, H. W. Turner, in PCT Int. Appl. W/O 91/09882, Exxon Chemical Co., **1991**; c) H. W. Turner, in Eur. Pat. Appl. EP 0277004A1, Exxon Chemical Co., **1988**.
[9] P. Jutzi, C. Muller, A. Stammler, H.-G. Stammler, *Organometallics* **2000**, *19*, 1442–1444.
[10] a) D. A. Horton, J. de With, A. J. van der Linden, H. van de Weg, *Organometallics* **1996**, *15*, 2672–2674; b) D. A. Horton, J. de With, *Organometallics* **1997**, *16*, 5424–5436.
[11] X. Bei, D. C. Swenson, R. F. Jordan, *Organometallics* **1997**, *16*, 3282–3302.
[12] J. C. W. Chien, W.-M. Tsai, M. D. Rausch, *J. Am. Chem. Soc.* **1991**, *113*, 8570–8571.
[13] Although arene interactions with by-product Ph_3CCH_3 have been claimed,[a] they have since been disproven.[b] a) C. P. Casey, D. W. Carpenetti, II, *J. Organomet. Chem.* **2002**, *642*, 120–130; b) S. J. Lancaster, M. Bochmann, *J. Organomet. Chem.* **2002**, *654*, 221–223.
[14] a) S. Beck, S. Lieber, F. Schaper, H.-H. Brintzinger, *J. Am. Chem. Soc.* **2001**, *123*, 1483–1489; b) F. Schaper, A. Geyer, H.-H. Brintzinger, *Organometallics* **2002**, *21*, 473–483; c) M.-C. Chen, T. J. Marks, *J. Am. Chem. Soc.* **2001**, *123*, 11803–11804; d) G. Lanza, I. L. Fragalà, T. J. Marks, *J. Am. Chem. Soc.* **2000**, *122*, 12764–12777; e) G. Lanza, I. L. Fragalà, T. J. Marks, *J. Am. Chem. Soc.* **1998**, *120*, 8257–8258.
[15] Models for SSIPs utilizing strong donors to disrupt the anion/cation contact are common.
[16] M. S. Chan, K. Vanka, C. C. Pye, T. Ziegler, *Organometallics* **1999**, *18*, 4624–4636.
[17] G. Lanza, I. L. Fragalà, T. J. Marks, *Organometallics* **2002**, *21*, 5594–5612.
[18] a) P. M. Zeimentz, S. Arndt, B. R. Elvidge, J. Okuda, *Chem. Rev.* **2006**, *106*, 2404–2433; b) W. E. Piers, D. J. H. Emslie, *Coord. Chem. Rev.* **2002**, *233–234*, 131–155; c) S. Arndt, J. Okuda, *Adv. Synth. Catal.* **2005**, *347*, 339–354.
[19] P. G. Hayes, L. W. M. Lee, L. K. Knight, W. E. Piers, M. Parvez, M. R. J. Elsegood, W. Clegg, R. MacDonald, *Organometallics* **2001**, *20*, 2533–2544.
[20] L. W. M. Lee, W. E. Piers, M. R. J. Elsegood, W. Clegg, M. Parvez, *Organometallics* **1999**, *18*, 2947–2949.
[21] a) P. G. Hayes, W. E. Piers, R. McDonald, *J. Am. Chem. Soc.* **2002**, *124*, 2132–2133; b) P. G. Hayes, W. E. Piers, M. Parvez, *Organometallics* **2005**, *24*, 1173–1183.
[22] P. G. Hayes, W. E. Piers, M. Parvez, *J. Am. Chem. Soc.* **2003**, *125*, 5622–5623.
[23] M. W. Bouwkamp, J. de Wolf, I. del Hierro Morales, J. Gercama, A. Meetsma, S. I. Troyanov, B. Hessen, J. H. Teuben, *J. Am. Chem. Soc.* **2002**, *124*, 12956–12957.
[24] a) C. A. Reed, K.-C. Kim, E. S. Stoyanov, D. Stasko, F. S. Tham, L. J. Mueller, P. D. W. Boyd, *J. Am. Chem. Soc.* **2003**, *125*, 1796–1804; b) C. A. Reed, N. L. P. Fackler, K.-C. Kim, D. Stasko, D. R. Evans, *J. Am. Chem. Soc.* **1999**, *121*, 6314–6315.
[25] R. D. Taylor, J. E. Kilpatrick, *J. Chem. Phys.* **1955**, *23*, 1232–1237.
[26] K. K. Kelley, *J. Am. Chem. Soc.* **1929**, *51*, 2738–2741.
[27] It should be noted that, according to our numbers, the highest barrier process for the k_{-1} direction is the conversion of η^n-**1e** to η^6-**1e**, although the energy of **A** is very close in energy to this transition state. In any case, the η^n-**1e** to η^6-**1e** conversion should also have a negative $\Delta S^{\neq}$.
[28] a) K. J. Klabunde, B. B. Anderson, M. Bader, L. J. Radonovich, *J. Am. Chem. Soc.* **1978**, *100*, 1313–1314; b) T. G. Traylor, M. J. Goldberg, *Organometallics* **1987**, *6*, 2531–2536; c) T. Takahashi, S. Hashiguchi, K. Kasuga, J. Tsuji, *J. Am. Chem. Soc.* **1978**, *100*, 7425–7427; d) R. G. Gastinger, B. B. Anderson, K. J. Klabunde, *J. Am. Chem. Soc.* **1980**, *102*, 4959–4966; e) A. C. Sievert, E. L. Muetterties, *Inorg. Chem.* **1981**, *20*, 489–501; f) M. M. Brezinski, K. J. Klabunde, *Organometallics* **1983**, *2*, 1116–1123; g) J. J. Harrison, *J. Am. Chem. Soc.* **1984**, *106*, 1487–1489; h) T. G. Traylor, K. J. Stewart, M. J. Goldberg, *J. Am. Chem. Soc.* **1984**, *106*, 4445–4454; i) T. G. Traylor, K. Stewart, *Organometallics* **1984**, *3*, 325–327; j) T. G. Traylor, K. J. Stewart, M. J. Goldberg, *Organometallics* **1986**, *5*, 2062–2067; k) T. G. Traylor, K. J. Stewart, *J. Am. Chem. Soc.* **1986**, *108*, 6977–6985; l) B. F. Bush, V. M. Lynch, J. J. Lagowski, *Organometallics* **1987**, *6*, 1267–1275; m) E. P. Kündig, V. Desobry, C. Grivet, B. Rudolph, S. Spichiger, *Organometallics* **1987**, *6*, 1173–1180; n) C. A. Sassano, C. A. Mirkin, *J. Am. Chem. Soc.* **1995**, *117*, 11379–11380; o) E. T. Singewald, X. Shi, C. A. Mirkin, S. J. Schofer, C. L. Stern, *Organometallics* **1996**, *15*, 3062–3069; p) M. F. Semmelhack, A. Chlenov, L. Wu, D. Ho, *J. Am. Chem. Soc.* **2001**, *123*, 8438–8439; q) C. S. Branch, A. R. Barron, *J. Am. Chem. Soc.* **2002**, *124*, 14156–14161.
[29] a) D. J. Gillis, R. Quyoum, M.-J. Tudoret, Q. Y. Wang, D. Jeremic, A. W. Roszak, M. C. Baird, *Organometallics* **1996**, *15*, 3600–3605; b) D. J. Gillis, M.-J. Tudoret, M. C. Baird, *J. Am. Chem. Soc.* **1993**, *115*, 2543–2545; c) S. J. Lancaster, O. B. Robinson, M. Bochmann, S. J. Coles, M. B. Hursthouse, *Organometallics* **1995**, *14*, 2456–2462.
[30] A. S. Guram, R. F. Jordan, *Organometallics* **1991**, *10*, 3470–3479.
[31] K. M. Doxsee, J. J. J. Juliette, J. K. M. Mouser, K. Zientara, *Organometallics* **1993**, *12*, 4682–4686.
[32] See Supporting Information for representative kinetic and Eyring plots.
[33] W. D. Cotter, J. E. Bercaw, *J. Organomet. Chem.* **1991**, *417*, C1–C6.
[34] B. J. Burger, M. E. Thompson, W. D. Cotter, J. E. Bercaw, *J. Am. Chem. Soc.* **1990**, *112*, 1566–1577.
[35] K. Vanka, M. S. W. Chan, C. C. Pye, T. Ziegler, *Organometallics* **2000**, *19*, 1841–1849.
[36] B. J. Burger, J. E. Bercaw, *Experimental Organometallic Chemistry*, American Chemical Society, Washington, D.C., **1987**.
[37] A. B. Pangborn, M. A. Giardello, R. H. Grubbs, R. K. Rosen, F. J. Timmers, *Organometallics* **1996**, *15*, 1518–1520.
[38] R. H. Marvich, H.-H. Brintzinger, *J. Am. Chem. Soc.* **1971**, *93*, 2046–2048.
[39] C. L. Perrin, T. J. Dwyer, *Chem. Rev.* **1990**, *90*, 935–967.
[40] *NMR and the Periodic Table* (Eds.: R. K. Harris, B. E. Mann), Academic Press, New York, **1978**.
[41] C. Ammann, P. Meier, A. E. Merbach, *J. Magn. Reson.* **1982**, 46–54.
[42] P. H. M. Budzelaar, A. B. van Oort, A. G. Orpen, *Eur. J. Inorg. Chem.* **1998**, 1485–1494.
[43] L. E. Manzer, *Inorg. Synth.* **1982**, *21*, 135–146.

Received: July 26, 2006
Published online: December 15, 2006

